Postprint of: Żołnowska B., Sławiński J., Szafrański K., Angeli A., Supuran C. T., Kawiak A., Wieczór M., Zielińska J., Bączek T., Bartoszewska S., Novel 2-(2-arylmethylthio-4-chloro-5-methylbenzenesulfonyl)-1-(1,3,5-triazin-2-ylamino)guanidine derivatives: Inhibition of human carbonic anhydrase cytosolic isozymes I and II and the transmembrane tumor-associated isozymes IX and XII, anticancer activity, and molecular modeling studies, European Journal of Medicinal Chemistry, Vol. 143 (2018), pp. 1931-1941, DOI: 10.1016/j.ejmech.2017.11.005

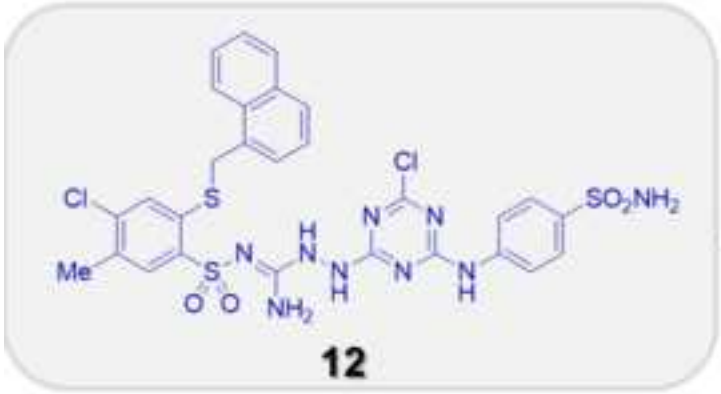

12

CYTOTOXICITY
Cervical **HeLa** cancer cells
IC_{50} = **17±1 μM**
Non-tumor HaCaT cells
IC_{50} = 61±8 μM

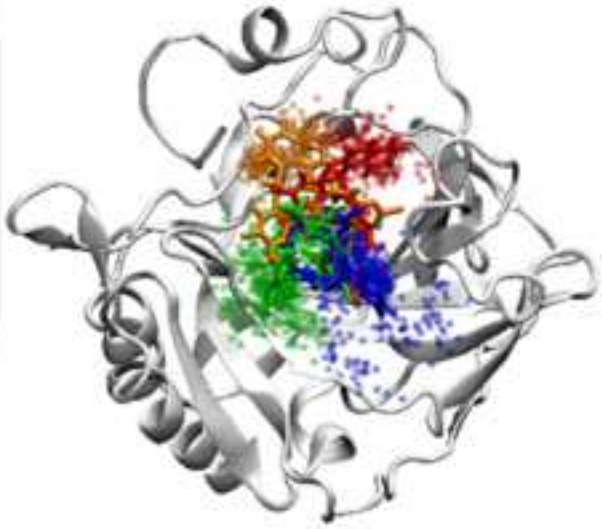

Transmembrane tumor-associated hCA IX isoform

K_I = 41.1 nM

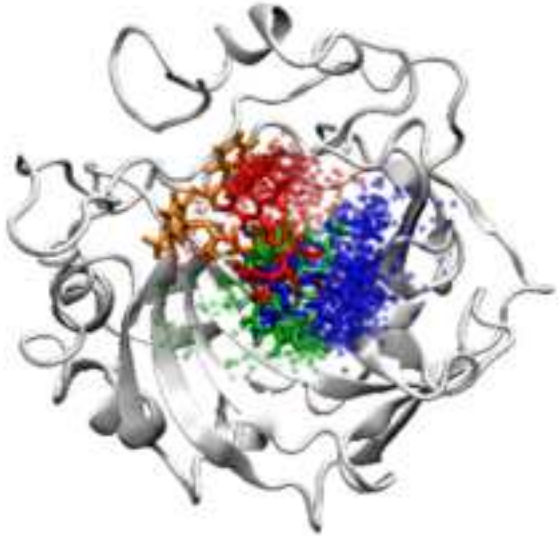

Cytosolic ubiquitous hCA II isoform

K_I = 160.8 nM

Original article

Novel 2-(2-arylmethylthio-4-chloro-5-methylbenzenesulfonyl)-1-(1,3,5-triazin-2-ylamino)guanidine derivatives: inhibition of human carbonic anhydrase cytosolic isozymes I and II and the transmembrane tumor-associated isozymes IX and XII, anticancer activity, and molecular modeling studies

Beata Żołnowska [a*], Jarosław Sławiński [a*], Krzysztof Szafrański [a], Andrea Angeli [b,c], Claudiu T. Supuran [b,c], Anna Kawiak [d,e], Miłosz Wieczór [f], Joanna Zielińska [g], Tomasz Bączek [g], Sylwia Bartoszewska [h]

[a] Department of Organic Chemistry, Medical University of Gdańsk, Al. Gen. J. Hallera 107, 80-416 Gdańsk, Poland
[b] Dipartimento di Chimica, Universita degli Studi di Firenze, Polo Scientifico, Laboratorio di Chimica Bioinorganica, Rm. 188, Via della Lastruccia 3, 50019 Sesto Fiorentino (Florence), Italy
[c] Università degli Studi di Firenze, NEUROFARBA Dept., Sezione di Scienze Farmaceutiche, 50019 Sesto Fiorentino (Florence), Italy
[d] Department of Biotechnology, Intercollegiate Faculty of Biotechnology, University of Gdańsk and Medical University of Gdańsk, ul. Abrahama 58, 80-307 Gdańsk, Poland
[e] Laboratory of Human Physiology, Medical University of Gdańsk, ul. Tuwima 15, 80-210 Gdańsk, Poland
[f] Department of Physical Chemistry, Gdańsk University of Technology, ul. Narutowicza 11/12, 80-233 Gdańsk, Poland
[g] Department of Pharmaceutical Chemistry, Medical University of Gdańsk, Al. Gen. J. Hallera 107, 80-416 Gdańsk, Poland
[h] Department of Inorganic Chemistry, Medical University of Gdańsk, Al. Gen. J. Hallera 107, 80-416 Gdańsk, Poland

ABSTRACT

A series of novel 2-(2-arylmethylthio-4-chloro-5-methylbenzenesulfonyl)-1-(6-substituted-4-chloro-1,3,5-triazin-2-ylamino)guanidine derivatives **9–20** have been synthesized by substitution of chlorine atom at the 1,3,5-triazine ring in compounds **5–8** with 3- or 4-aminobenzenesulfonamide and 4-(aminomethyl)benzenesulfonamide hydrochloride. All the synthesized compounds were evaluated for their inhibitory activity toward hCA I, II, IX and XII as well as anticancer activity against HeLa, HCT-116 and MCF-7 human tumor cell lines. The investigated compounds showed weak inhibitory potency against the human CA I, while activity toward hCA II was differentiated and depended on structure of inhibitor (K_I: 5.4–933.1 nM). Compounds containing the 4-sulfamoylphenyl moiety (**9**–**12**) exhibited the strongest inhibitory activity against hCA IX with K_I values from 37.1 to 42.9 nM, as well as against hCA XII in range of 31–91.9 nM. The most promising compound **12** (K_I = 41 nM) showed the highest selectivity toward hCA IX versus hCA I (hCA I/hCA IX = 18) and hCA II (hCA II/hCA IX = 4). Compound **12** displayed prominent cytotoxic effect selectively toward HeLa cancer cells (IC_{50} = 17 μM) and did not exhibit toxicity to the non-cancerous HaCaT cells. *In silico* analysis suggested that despite the lack of a single binding pose, the selective affinity is conferred by specific interactions with an arginine moiety, as well as better-defined binding modes within the active site.

Keywords: Benzenesulfonamide; Synthesis; Anticancer; Carbonic anhydrase Inhibitors; Molecular dynamics

*Corresponding authors. Tel.: +48 58 349 12 29; fax: +48 58 349 12 77.
E-mail addresses: zolnowska@gumed.edu.pl (B. Żołnowska), jaroslaw@gumed.edu.pl (J. Sławiński).

1. Introduction

Carbonic anhydrases (CAs, EC 4.2.1.1) are zinc-containing metalloenzymes that participate in the maintenance of pH homeostasis in the body by catalyzing the reversible hydration of carbon dioxide to bicarbonate ions and protons ($CO_2 + H_2O \leftrightarrow HCO_3^- + H^+$) [1]. So far, 16 isoforms of carbonic anhydrase have been characterized in mammals that differ in their subcellular localization, catalytic activity and susceptibility to different classes of inhibitors [2,3]. Among these isoforms, the human cytosolic isoforms hCA I and hCA II are ubiquitous in the body and are involved in the secretion of electrolytes in a multitude of tissues, such as the bicarbonate rich aqueous humor in the anterior chamber of the eyes or the cerebrospinal fluid, as well as maintain pH and CO_2 homeostasis all over the body [4]. However, dysregulation of activity of hCA I and II in tissues leads to pathologic conditions, such as glaucoma or edema [4]. Therefore, hCA I and II became targets for anticonvulsant, diuretic and anti-glaucoma drugs [5]. In contrast, isozymes hCA IX and XII have been recognized as the extracellular membrane-bound CAs associated with tumor progression and metastases formation [6]. hCA IX, expressed in several types of human carcinomas, was also found in a very limited number of normal tissues, such as gastrointestinal mucosa and gastrointestinal related structures [7]. hCA XII, which was first found in normal kidney tissue and renal cell carcinoma, in later studies was discovered in several other tumors as well as in some normal organs such as the colon and uterus [8].

The main function of hCA IX is to maintain pH homeostasis under hypoxic conditions that are common in solid tumors, although it is also involved in intercellular communication *via* the N-terminal proteoglycan-like region (PG) that has been implicated in cell adhesion [9]. hCA IX functions as an important ion transporter and pH regulator by forming a bicarbonate transport metabolon with the sodium bicarbonate transporter NBCe1 and anion exchanger 2 (AE2) that are both components of the migration apparatus [10]. CA IX physically interacts with AE2 and NBCe1 in situ, thus it is suggested that hCA IX actively contributes to cell migration via its ability to facilitate ion transport and pH control at protruding fronts of moving cells [10]. The expression of hCA IX is induced by hypoxic conditions under tight regulation by the hypoxia inducible factor 1 alpha (HIF1-α) that binds to the hypoxia response element (HRE) located next to the transcription initiation site [11]. hCA IX becomes enzymatically active when protein kinase A (PKA) phosphorylates Thr443 at the intracellular domain of hCA IX [12]. The general result of hCA IX overexpression in tumors is pH decrease in the extracellular microenvironment from pH ~ 7.4 (normal tissue) to pH ~ 6.8 (hypoxic tumor) that enhances tumor cell survival under hypoxic conditions and contributes to the evolution of metastatic and drug-resistant phenotypes [13–15]. Abnormally high

expression of hCA IX in tumors is documented as a marker of hypoxia and an indicator of poor prognosis [16]. The hCA IX became a clinically relevant target for anticancer treatment and its inhibition has been proposed as an attractive option for therapeutic targeting of various hypoxic tumors [17].

Classical carbonic anhydrase inhibitors (CAIs) belong to primary sulfonamides and are initially developed as diuretics and systemically acting antiglaucoma drugs **AAZ, MZA, DCP** and **EZA** (**Fig. 1**)[18]. Several CA isozymes are strongly inhibited at once by these compounds, including the tumor-associated isoforms hCA IX, hCA XII and the physiologically dominant cytosolic isoform hCA II. Thus, they have attracted little interest as anticancer agents [19]. Many approaches to achieve high selectivity toward hCA IX were reported over recent years as various sulfonamide, sulfamate, sulfamide, coumarin and Probenecid-based CAIs were discovered to efficiently target hCA IX [20, 21]. Among these inhibitors ureido sulfonamides gained particular importance owing to the clinical evaluations of SLC-0111 (**Fig.1**) [22]. Currently, SLC-0111 is involved in a phase I, Multi-center, Open-label, study (https://clinicaltrials.gov/ct2/show/NCT02215850) that aims to investigate its safety, tolerability, and pharmacokinetic and to gain some information about its effectiveness in treating cancer.

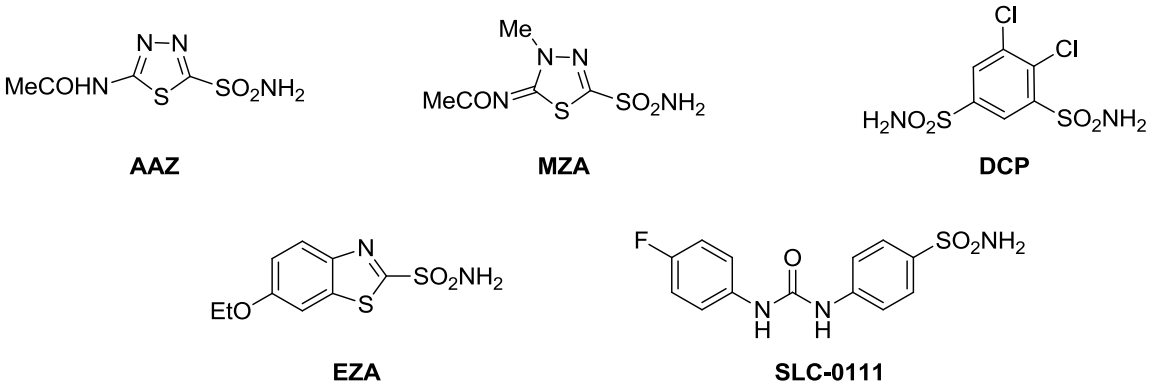

Fig. 1. General structures of clinically used sulfonamides **AAZ, MZA, DCP** and **EZA** (standard CA inhibitors) and sulfonamide SLC-0111, being in clinical trials.

In the last years it has been reported that novel triazinyl-containing CAIs, such as compounds **A1-A3** (**Fig. 2**), possess sub-nanomolar activity for the selective inhibition of the tumor-associated isoforms hCA IX and hCA XII [23–25]. Recently we have described the synthesis a number of sulfonamides of type **B** [26], **C** [27] and **D** [28] (see **Fig. 2**) and their inhibitory activities against isoforms hCA I, II, IX, XII. Taking into account our previous reports and the current knowledge about association between hCA IX overexpression and

tumors, we decided to investigate the inhibitory activity against CAs for the series of 2-(2-arylmethylthio-4-chloro-5-methylbenzenesulfonamide)-1-(1,3,5-triazin-2-ylamino)guanidines of type **E** (**Fig. 2**). We focused on discovery of hCA IX/XII-selective inhibitors (with selectivity for the tumor-associated isoforms IX and XII over the cytosolic ones I and II) whose activity might alleviate the side effects compared to clinically used anticancer agents.

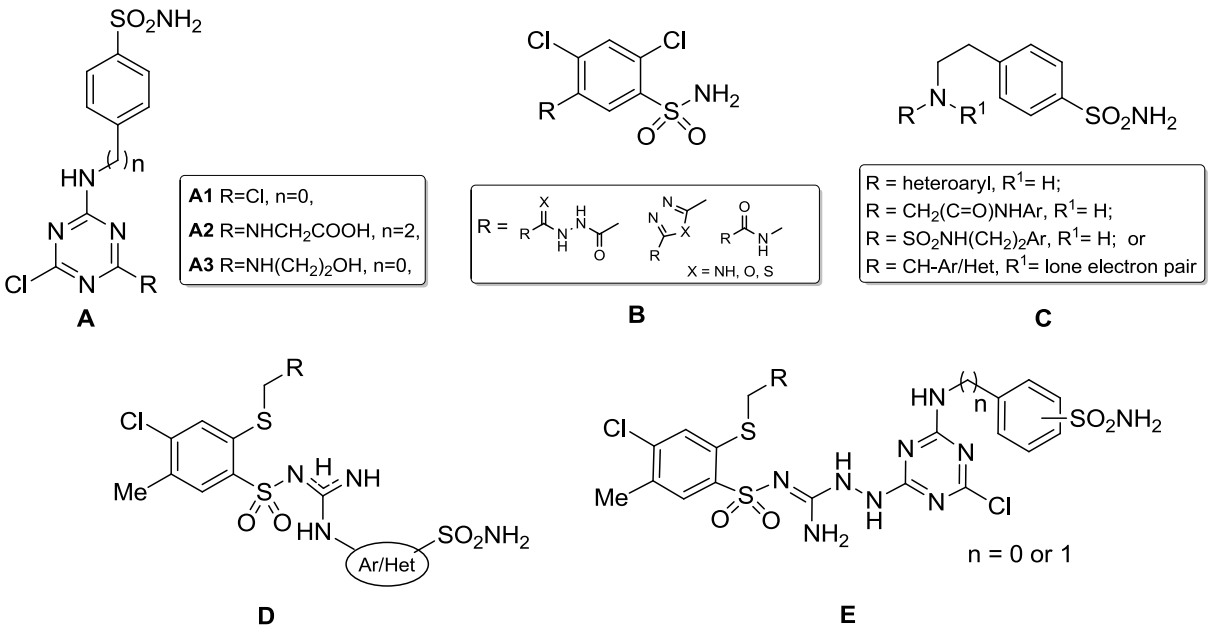

Fig 2. Structures of benzenesulfonamides **A**, **B**, **C, D** and **E**.

2. Results and discussion

2.1. Chemistry

Novel 2-(2-arylmethylthio-4-chloro-5-methylbenzenesulfonyl)-1-(4,6-dichloro-1,3,5-triazin-2-ylamino)guanidine derivatives **5–8** were synthesized by the reaction of appropriate aminoguanidine (**1–4**) with 2,4,6-trichloro-1,3,5-triazine in a presence of triethylamine under previously determined reaction conditions i.e. anhydrous tetrahydrofuran and 0 °C (Scheme 1). Starting aminoguanidines **1–4** were achieved according to procedures that we have described earlier [29–31]. In the second stage of synthesis, the final 2-(2-arylmethylthio-4-chloro-5-methylbenzenesulfonyl)-1-(6-substituted-4-chloro-1,3,5-triazin-2-ylamino)guanidines **9-20** were obtained by reaction of dichloro-substituted triazine derivatives **5–8** with one equivalent of amine nucleophile, such as 3- or 4-aminobenzenesulfonamide and 4-(aminomethyl)benzenesulfonamide hydrochloride. Nucleophilic substitution of second reactive chlorine atom at the 1,3,5-triazine ring was

carried out in dry DMF at 65–80 ºC under an argon atmosphere in the presence of DIPEA as a base (**Scheme 1**). The reactions proceeded for 3-11 h (reaction times were monitored using RP-HPLC method) with satisfactory yields. The structure of final compounds was confirmed by mass spectrometry and spectroscopic data (IR, ^{1}H NMR, ^{13}C NMR). ^{1}H NMR spectra in DMSO-d_6 revealed two singlets at range 6.94–7.26 ppm for NH_2 and SO_2NH_2, and distinctive three singlets at range 8.01–10.54 ppm for NH groups. All compounds were also identified by elemental analyses (C, H, N).

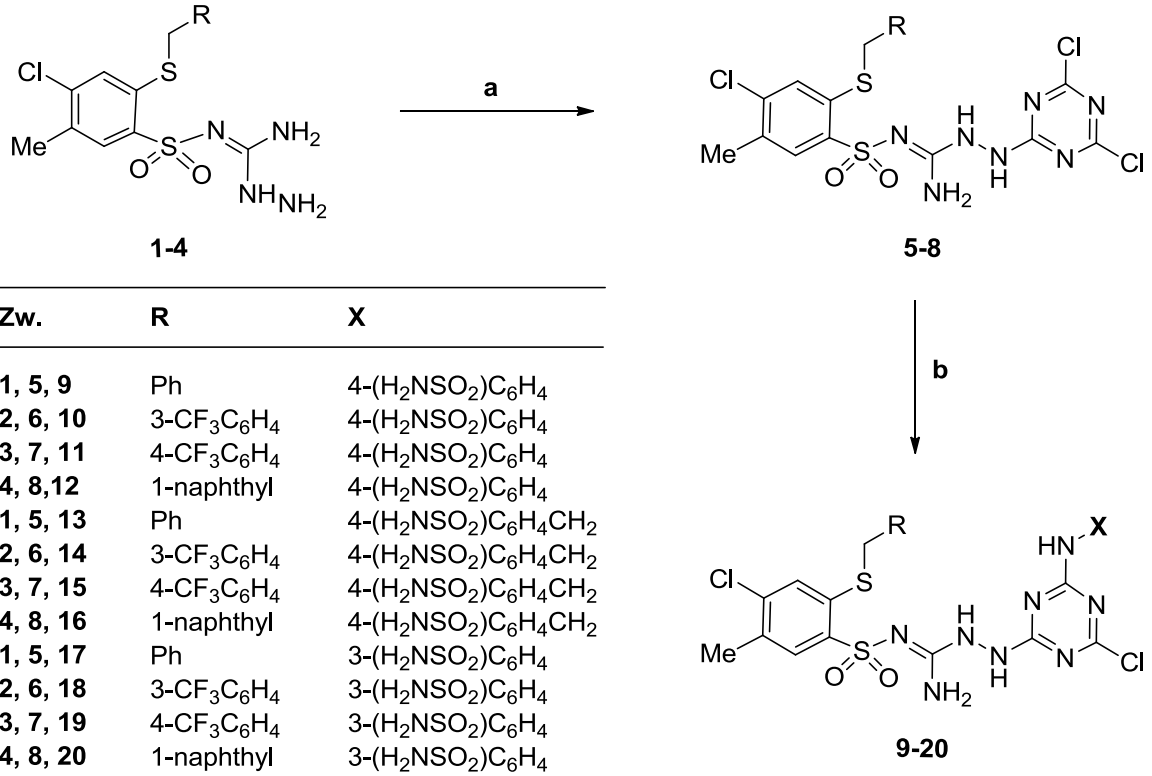

Zw.	R	X
1, 5, 9	Ph	4-(H_2NSO_2)C_6H_4
2, 6, 10	3-$CF_3C_6H_4$	4-(H_2NSO_2)C_6H_4
3, 7, 11	4-$CF_3C_6H_4$	4-(H_2NSO_2)C_6H_4
4, 8,12	1-naphthyl	4-(H_2NSO_2)C_6H_4
1, 5, 13	Ph	4-(H_2NSO_2)$C_6H_4CH_2$
2, 6, 14	3-$CF_3C_6H_4$	4-(H_2NSO_2)$C_6H_4CH_2$
3, 7, 15	4-$CF_3C_6H_4$	4-(H_2NSO_2)$C_6H_4CH_2$
4, 8, 16	1-naphthyl	4-(H_2NSO_2)$C_6H_4CH_2$
1, 5, 17	Ph	3-(H_2NSO_2)C_6H_4
2, 6, 18	3-$CF_3C_6H_4$	3-(H_2NSO_2)C_6H_4
3, 7, 19	4-$CF_3C_6H_4$	3-(H_2NSO_2)C_6H_4
4, 8, 20	1-naphthyl	3-(H_2NSO_2)C_6H_4

Scheme 1. Synthesis of 2-(2-arylmethylthio-4-chloro-5-methylbenzenesulfonyl)-1-(1,3,5-triazin-2-ylamino)guanidine **5-8** and **9-20**. Reagents and conditions: a) 2,4,6-trichloro-1,3,5-triazine (1 equiv.), TEA (1-2 equiv.), anhydrous THF, 1 h at 0 °C, 2 h at r.t.; b) X-NH_2 (1 equiv.), DIPEA (1 equiv.), 80°C, argon atmosphere, 3–11 h.

2.2. CA inhibition studies

Compounds **9-20** and standards, clinically used CAIs, such as acetazolamide **AAZ**, methazolamide **MZA**, ethoxzolamide **EZA** and dichlorophenamide **DCP** were screened for the inhibition of two cytosolic ubiquitous isozymes of human origin hCA I and hCA II, and transmembrane tumor-associated isoforms hCA IX and XII (**Table 1**). From the inhibition data reported in **Table 1**, the following findings can be noted:

1. An investigated series of sulfonamide derivatives turned out to be rather weak inhibitors of hCA I exhibiting K_I values in a range 66–3341 nM. Among them compound **9** with R = phenyl and X = 4-sulfamoylphenyl as substituents showed the highest affinity to the hCA I with K_I = 66 nM. However, change of **X** substituent in compound **9** into more bulky 4-sulfamoylbenzyl fragment (**13**) as well as into positional isomer – 4-sulfamoylphenyl moiety (**17**) significantly decreased this affinity.
2. Results of experiments on hCA II indicated lower inhibitory activity of investigated series then reference drugs, with the exception of compounds **10, 14** and **18** containing 3-trifluoromethylphenyl group at position R. These compounds showed strong inhibitory activity toward hCA II with K_I values from 5.4 to 9.3 nM, while **10** and **14** were stronger inhibitors then the most active reference hCA II inhibitor - **EZA** (K_I = 8 nM). High inhibitory activity of guanidine derivatives with R = 3-trifluoromethylphenyl residue decreased after exchange on isomeric 4-trifluoromethylphenyl as R substituent. It should be pointed out that the presence of bulky aromatic fragments at R, i.e. 1-naphthyl decreased inhibitory efficacy against hCA II remarkably (**12**, **16**, **20**; K_I in a range 160.8–933.1 nM).
3. Inhibitory activity toward hCA IX highly depends on structure of **X** substituent of tested compounds, that is supported by results given in **Table 1**. A series containing 4-sulfamoylphenyl moiety (**9**–**12**) presented the strongest inhibitory activity with K_I values from 37.1 to 42.9 nM, whereas series possessing isomeric 3-sulfamoylphenyl substituent (**17**–**20**) was inactive (K_I: 421.1–3968.7 nM). Extending of 4-sulfamoylphenyl residue by methylene group decreased activity of compounds **14** and **15** (R = 3- and 4-trifluoromethylphenyl, K_I: 43.6 and 47.1 nM**)** insignificantly, but in the case of compound **16** (R = 1-naphthyl) caused strong decline in activity (**16**, K_I = 383 nM).
4. Compounds **9–12** bearing 4-sulfamoylphenyl moiety as **X** revealed the highest ability to hCA XII inhibition with K_I values ranging from 31 to 91.9 nM. Taking into account results from **Table 1**, inhibitory activities of **9–12** were reduced by more than half after substitution of 4-sulfamoylbenzyl or 3-sulafmoylphenyl residue in **X** position.
5. It is worth to note that compound **12** exhibits the highest selectivity toward hCA IX versus hCA I (hCA I/hCA IX = 18) and hCA II (hCA II/hCA IX = 4) and

represents the most promising inhibitor targeting transmembrane tumor-associated isozyme such as hCA IX.

Table 1. Carbonic anhydrase inhibition data for compounds **9-20** and standard inhibitors against human isozymes hCA I, II, IX and XII by a stopped-flow CO_2 hydrase assay.

Compound	R	X	K_I[a] (nM)			
			hCA I	hCA II	hCA IX	hCA XII
AAZ			250	12.1	25.8	5.7
MZA			780	14	27	3.4
EZA			25	8	34	22
DCP			1200	38	50	50
9	Ph	4-(H_2NSO_2)C_6H_4	66.6	83.7	39.4	31.1
10	3-$CF_3C_6H_4$	4-(H_2NSO_2)C_6H_4	147.6	7.4	37.1	91.9
11	4-$CF_3C_6H_4$	4-(H_2NSO_2)C_6H_4	385.6	22.0	42.9	87.5
12	1-naphthyl	4-(H_2NSO_2)C_6H_4	733.3	160.8	41.1	77.6
13	Ph	4-(H_2NSO_2)$C_6H_4CH_2$	294.2	38.8	46.9	78.8
14	3-$CF_3C_6H_4$	4-(H_2NSO_2)$C_6H_4CH_2$	218.9	5.4	43.6	255.5
15	4-$CF_3C_6H_4$	4-(H_2NSO_2)$C_6H_4CH_2$	513.8	89.5	47.1	183.3
16	1-naphthyl	4-(H_2NSO_2)$C_6H_4CH_2$	2141.0	186.9	383.0	73.4
17	Ph	3-(H_2NSO_2)C_6H_4	395.9	94.7	3968.7	64.6
18	3-$CF_3C_6H_4$	3-(H_2NSO_2)C_6H_4	336.8	9.3	3342.1	225.8
19	4-$CF_3C_6H_4$	3-(H_2NSO_2)C_6H_4	536.1	326.2	421.1	392.8
20	1-naphthyl	3-(H_2NSO_2)C_6H_4	3341.0	933.1	3403.2	337.9

[a] Mean from 3 different determinations (errors were in the range of ±5-10% of the reported values, data not shown).

2.3. Cytotoxic activity

Compounds **9**–**20** were evaluated *in vitro* for their effects on the viability of three human cancer cell lines: HeLa (cervical cancer), HCT-116 (colon cancer) and MCF-7 (breast cancer). The concentration required for 50% inhibition of cell viability IC_{50} was calculated and as a positive control cisplatin was used. Analysis was performed using the MTT assay after 72 hours of incubation. Results of the tests indicated that all compounds except **12** were inactive (IC_{50} > 100 μM). Compound **12** exhibited cytotoxic activity against HeLa cell line with IC_{50} = 17±1 μM. To assess if the effect of **12**, shown toward HeLa cells, could be related to a selected cytotoxicity or to more general toxic effect, assay on the non-tumor cell line HaCaT (immortalized human keratinocytes) was performed. An investigation indicated that compound showed selectivity toward cancer cells. The values of IC_{50} = 61±8 μM for HaCaT displayed about 3.6 times less toxicity than that for HeLa cells.

2.4. Molecular dynamics simulations

To investigate the molecular origin of selectivity of the obtained compounds towards the hCA IX vs hCA II isoform, as well as rationalize the impact of substituents on the binding affinity, we employed an *in silico* model of the protein-ligand complex. For the computational study, two compounds were chosen: compound **12** as the ligand with highest selectivity for hCA IX, and compound **20** since it expressed a large difference in binding affinity resulting from a minor difference in structure (*meta*- vs *para*- substitution). First, it was used steered Molecular Dynamics (MD) to obtain the initial geometry of the ligand tethered to the enzyme active site. To this end, the distance between the sulfonamide nitrogen and the zinc cofactor was gradually restrained, as motivated by the review of known sulfonamide-anhydraze complexes [32–34]. The high conformational flexibility of the elongated ligand molecule prompted us to use the replica exchange metadynamics enhanced sampling method (see Methods) to sample all possible geometries of the protein-ligand complex in all 4 available combinations. The visualization of thus obtained ensembles revealed the existence of multiple binding poses, shown for compound **12** in **Fig. 3A**, suggesting that the protein-ligand complex does not assume a single well-defined geometry, instead interacting transiently with multiple – often hydrophobic – patches on the protein surface.

For this reason, we focused on the identification of stable poses that explain the observed differences in affinity. We used K-means clustering to find distinct poses assumed by the ligands, and optimized the number of clusters with respect to the K-means objective function (Fig. S1). The results suggested that 4 binding poses can be meaningfully assigned in case of hCA IX; in contrast, an optimal cluster number could not be as easily determined for complexes of compounds **12** and **20** with hCA II, suggesting that the selectivity towards hCA IX in case of compound **12** can be partially explained by the conformational promiscuity of hCa II-bound ligand lacking distinct binding poses.

In order to assess the stability of the identified binding poses, for each protein-ligand pair, additional 250-ns equilibrium simulations seeded from the frames closest to the cluster centers was run. As seen in **Fig. 3B**, in case of compound **12** bound to hCA IX (12/IX), three of four bound ligands remained within their initial clusters over the entire simulation, indicating that the identified binding poses are stable and did not merely arise as artifacts of the enhanced sampling. Interestingly, the stability of identified poses in the equilibrium simulations clearly correlates with experimentally determined binding affinities, with the 12/IX pair characterized by highest affinity and followed by 12/II (two interchanging poses), 20/II and 20/IX (3-4 rapidly interchanging poses).

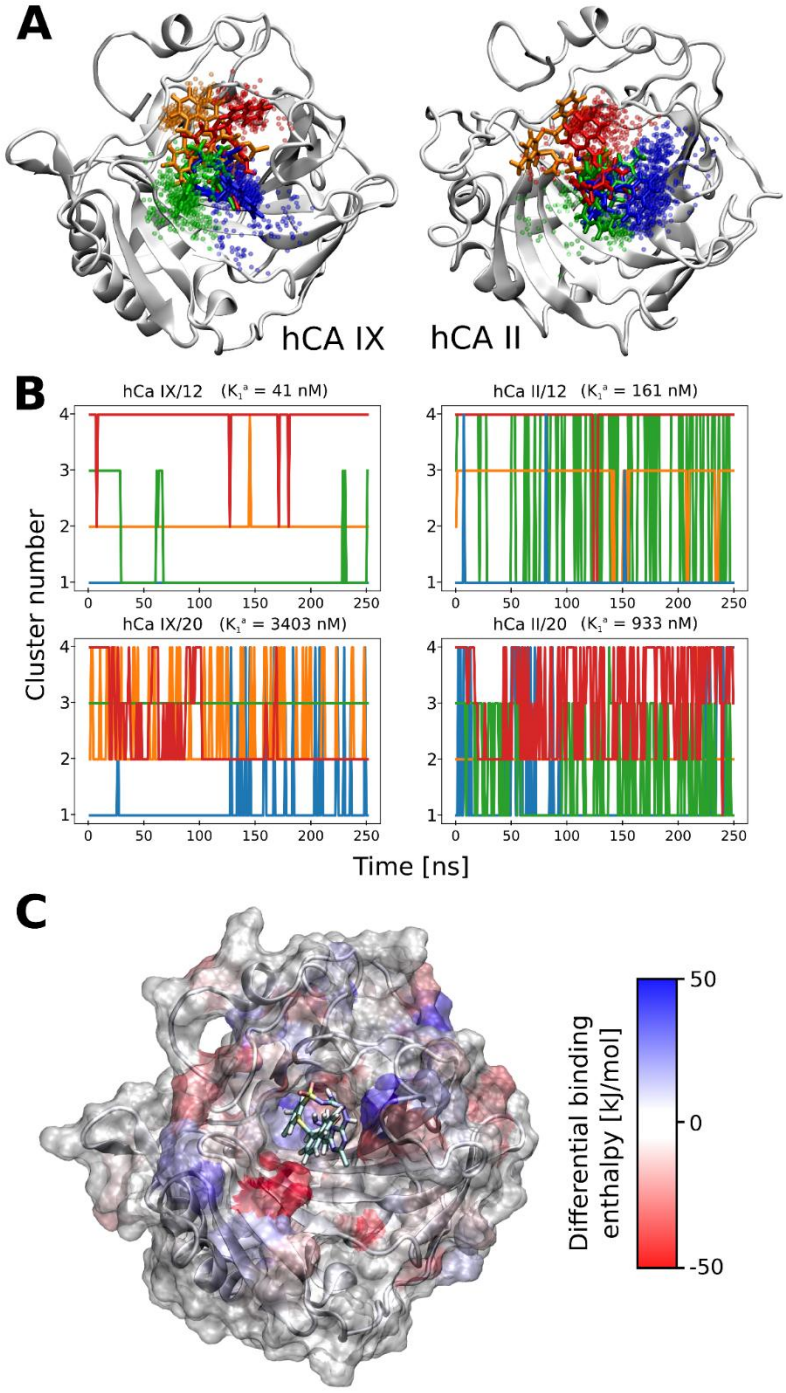

Fig. 3. (**A**) The binding poses identified for compound **12** by the clustering procedure, with cluster centers (shown in the stick representation) and cluster members (shown as transparent spheres corresponding to the position of the naphthyl moiety). (**B**) Stability of identified binding poses in 250 ns equilibrium simulations. Fewer transitions between unstable poses correlate with higher affinity as determined experimentally. (**C**) Difference in binding enthalpy between compound **12** and the corresponding (according to the BLAST alignment) amino acids of hCA IX and II, mapped onto the protein structure. Red indicates higher binding enthalpy in case of hCA IX, blue – in case of hCA II.

As the reliability our structural description is crucially dependent on whether it complies with experimental data, we used thermodynamic integration (TI) to calculate the difference in binding affinity for hCA IX between compounds **12** and **20** and obtained a value of 2.0 kcal/mol, in qualitative and quantitative agreement with the experimental result (2.6 kcal/mol calculated from the data in **Table 1**). We note that for highly flexible ligands such as considered here, TI fared superior to more approximate binding affinity determination methods such as MM-PBSA and plain rigid-body docking, both of which delivered qualitatively wrong results.

Finally, to identify the regions that likely contribute to the observed selectivity of compound **12** towards hCA IX, we decomposed the interaction enthalpy from the enhanced sampling simulations to calculate the enthalpic contribution of individual amino acids to the binding affinity. This task is not straightforward due to relatively low sequence identity between the two isoforms, and hence sequence alignment was performed first to identify corresponding regions in both proteins. Then the difference in mean ligand-amino acid interaction enthalpies was calculated for the corresponding amino acids and color-mapped onto the protein structure to obtain a spatially resolved differential affinity map. The results, shown in **Fig. 3C**, indicate that the observed selectivity plausibly derives mostly from the interaction with the β-sheet region of the protein. A closer inspection of the trajectories revealed that this enthalpic difference is indeed reflected in frequent π- π type association of the naphthyl and/or phenyl ring of compound **12** with the planar guanidine moiety of Arg64 (Fig. S2), an interaction that is absent in case of hCA II where this residue is substituted with Leu57. We note that even though enthalpic analysis cannot account for the (inherently non-local) entropic contribution, often crucial in predicting hydrophobic affinity, that this approach can prove useful in further development of more selective ligands by locating specific sites on the protein surface that accommodate the respective substituents more easily in case of hCA IX than hCA II.

3. Conclusions

We have synthesized a series of novel 2-(2-arylmethylthio-4-chloro-5-methylbenzenesulfonyl)-1-[4-chloro-6-(4-sulfamoylphenylamino)-1,3,5-triazin-2-ylamino]guanidine and 2-(2-arylmethylthio-4-chloro-5-methylbenzenesulfonyl)-1-[4-chloro-6-(4-sulfamoylphenylmethylamino)-1,3,5-triazin-2-ylamino]guanidine derivatives. All compounds were investigated for their inhibitory activity toward two cytosolic ubiquitous

isozymes of human origin hCA I and hCA II, and transmembrane tumor-associated isoforms hCA IX and XII. Compounds showed rather weak inhibitory potency against hCA I, while toward hCA II the activity was differentiated and depended on structure of inhibitor. The most active inhibitors of hCA II was the series with R = 3-trifluoromethylphenyl group, whereas series with 1-naphthyl as R substituent turned out weak inhibitors of this isoform. On the other hand, compound with 1-naphthyl moiety (**12**) exhibited high affinity to hCA IX (K_I = 41.1 nM) that was the desired feature in this work. Moreover, compound **12** showed the highest selectivity toward hCA IX versus hCA I (hCA I/hCA IX = 18) and hCA II (hCA II/hCA IX = 4) and represented the most promising inhibitor targeting transmembrane tumor-associated isozyme such as hCA IX. hCA XII, second extracellular membrane-bound carbonic anhydrase associated with tumor progression was inhibited by compounds bearing 4-sulfamoylphenyl moiety (**9**–**12**) with K_I values ranging from 31 to 91.9 nM. It has been also found in our work that compound **12** displayed prominent cytotoxic effect selectively toward HeLa cancer cells (IC_{50} = 17 μM) and did not exhibit toxicity to the non-cancerous HaCaT cells (IC_{50} = 61 μM).

Employing an *in silico* model of the protein-ligand complex, the molecular origin of selectivity of compound **12** towards the hCA IX vs hCA II isoform was investigated. Identification of stable poses for complex **12** and hCA IX suggested the selectivity towards hCA IX can be partially explained by the conformational promiscuity of hCA II-bound ligand **12** lacking distinct binding poses. We also identified the regions that likely contribute to the observed selectivity of compound **12** towards hCA IX. The most important interaction was π-π type association of the naphthyl and/or phenyl ring of compound **12** with the planar guanidine moiety of Arg64, an interaction that was absent in case of hCA II where this residue is substituted with Leu57.

4. Experimental protocols

4.1. Synthesis

Melting points were uncorrected and measured using Thermogalen (Leica) apparatus. IR spectra were measured on Thermo Mattson Satellite FTIR spectrometer in KBr pellets; an absorption range was 400-4000 cm^{-1}. ^1H NMR and ^{13}C NMR spectra were recorded on a Varian Gemini 200 apparatus or Varian Unity Plus 500 apparatus. Chemical shifts are expressed at δ values relative to Me_4Si (TMS) as an internal standard. The apparent resonance

multiplicity is described as: s (singlet), d (doublet), t (triplet) and m (multiplet). Elemental analyses were performed on PerkinElmer 2400 Series II CHN Elemental Analyzer and the results indicated by the symbols of the elements were within ± 0.4 % of the theoretical values. Thin-layer chromatography (TLC) was performed on Merck Kieselgel 60 F254 plates and visualized with UV. Gravity liquid chromatography was conducted using silica gel with pore size 60 Å, 220-440 mesh particle size, 35-75 μm particle size or aluminum oxide with pore size 58 Å, activated, neutral, pH=7 (in H_2O) and a mixture of CH_2Cl_2/MeOH or $CHCl_3$/MeOH as the eluents. Purity of compounds was analyzed by RP-HPLC on Shimadzu (Model LC-10AD) HPLC system; Column: Gemini 4.6 x 250 mm; C6-phenyl; 5μm; 110 Å, Mobile Phase: A – grade water with 0.1% (v/v) trifluoroacetic acid, B – 80% acetonitrile-water containing 0.08% (v/v) trifluoroacetic acid, linear gradient 5–100% B in 45 min, Flow Rate: 1 ml/min. The purity of compounds was >95%, as determined by RP-HPLC. High resolution mass spectrometry (HRMS) were performed on TripleTOF® 5600+ mass spectrometer (AB SCIEX, Framingham, MA, USA) equipped with a DuoSpray™ Ion Source and coupled with Micro HPLC system Ekspert™ microLC 200 (Eksigent Redwood City, CA, USA); Column: HALO Fused-Core C18 (50 x 0.5 mm, 2.7 μm) (Eksigent), thermostated at 50°C; Flow: 30 μl/min; Mobile Phase: A: 0.1% formic acid in water, B: 0.1% formic acid in acetonitrile; Isocratic program 100%B, 4 min.

The commercially unavailable 1-amino-2-(4-chloro-5-R^1-2-alkylthiobenzenesulfonyl)guanidines were obtained according to the following methods described previously: **1** [29], **2–3** [30], **4** [31].

4.1.1. General procedure for the synthesis of 2-(2-arylmethylthio-4-chloro-5-methylbenzenesulfonyl)-1-(4,6-dichloro-1,3,5-triazin-2-ylamino)guanidines **(5–8)**

To a stirred solution of 2,4,6-trichloro-1,3,5-triazine (0.553 g, 3 mmol) in THF (12 ml) at 0 °C an aminoguanidine (3 mmol) was added in portions during 1 h. The reaction mixture was stirred at 0 °C for 30 min and then TEA (0.417 ml, 3 mmol) was added dropwise. Stirring was continued for 2 h at room temperature. After reaction solvent was evaporated under reduced pressure and the residue was suspended in ice slush (50 ml). The solid was filtered off, washed with water, dried and purified as indicated below.

*4.1.1.1. 2-(2-Benzylthio-4-chloro-5-methylbenzensulfonyl)-1-(4,6-dichloro-1,3,5-triazin-2-ylamino)guanidine (**5**)*

Starting with **1** (2.124 g) and after crystallization from acetone/water the title compound **5** was afforded 1.259 g (78.8%): m.p. 227–229 ºC; t_R= 49.27 min; IR (KBr) ν_{max} 3419, 3319, 3210 (N-H); 2925, 2852 (CH_3); 1649, 1538 (C=N, C=C); 1386 ($SO_{2\ asym}$); 1134, 1181 ($SO_{2\ sym}$) cm^{-1}; ^1H NMR (500 MHz, DMSO-d_6, 50 ºC) δ 2.33 (s, 3H, CH_3), 4.26 (s, 2H, SCH_2), 7.08 (s, 2H, NH_2), 7.23 (t, 1H, arom), 7.30 (t, 2H, arom), 7.36-7.43 (m, 3H, arom), 7.86 (s, 1H, NH), 9.42 (s, 1H, NH), 10.78 (s, 1H, NH) ppm; HRMS (ESI-TOF) *m/z* calcd for $C_{18}H_{16}Cl_3N_7O_2S_2$ $[M+H]^+$ 531.9951, found 531.9935. Anal. ($C_{18}H_{16}Cl_3N_7O_2S_2$) C, H, N.

*4.1.1.2. 2-[4-Chloro-5-methyl-2-(3-trifluoromethylbenzylthio)benzenesulfonyl]-1-(4,6-dichloro-1,3,5-triazin-2-ylamino)guanidine (**6**)*

Starting with **2** (1.359 g) and after crystallization from chloroform/methanol (v/v = 16:3) the title compound **6** was afforded 1.359 g (75%): m.p. 126–129 ºC, $t_{R=}$ 45.17 min; IR (KBr) ν_{max} 3421, 3313 (N-H); 2926 (CH); 1633, 1545 (C=N, C=C); 1383, 1325 ($SO_{2\ asym}$); 1128 ($SO_{2\ sym}$) cm^{-1}; ^1H NMR (500 MHz, DMSO-d_6, 50 ºC) δ 2.30 (s, 3H, CH_3), 4.38 (s, 2H, SCH_2), 7.24 (s, 2H, NH_2), 7.39 (s, 1H, arom), 7.55 (t, 1H, arom), 7.58 (d, 1H, arom), 7.72 (s, 2H, arom), 7.85 (s, 1H, arom), 9.48 (s, 1H, NH), 10.78 (s, 1H, NH) ppm; HRMS (ESI-TOF) *m/z* calcd for $C_{19}H_{15}Cl_3F_3N_7O_2S_2$ $[M+H]^+$ 599.9825, found 599.9810. Anal. ($C_{19}H_{15}Cl_3F_3N_7O_2S_2$) C, H, N.

*4.1.1.3. 2-[4-Chloro-5-methyl-2-(4-trifluoromethylbenzylthio)benzenesulfonyl]-1-(4,6-dichloro-1,3,5-triazin-2-ylamino)guanidine (**7**)*

Starting with **3** (1.359 g) and after crystallization from acetone/water the title compound **7** was afforded 1.521 g (84%): m.p. 122–124 ºC; $t_{R=}$ 45.76 min; IR (KBr) ν_{max} 3421, 3313 (N-H); 2926 (CH); 1633, 1545 (C=C, C=N); 1383, 1325 (SO_{2asym}); 1128 ($SO_{2\ asym}$); 1134 ($SO_{2\ sym}$) cm^{-1}; ^1H NMR (500 MHz, DMSO-d_6, 100 ºC) δ 2.29 (s, 3H, CH_3), 4.32 (s, 2H, SCH_2), 7.20 (s, 2H, NH_2 exchanged with D_2O), 7.35 (s, 1H, arom), 7.57 (d, 4H, arom), 7.85 (s, 1H, arom), 9.60 (s, 1H, NH exchanged with D_2O), 10.79 (s, 1H, NH exchanged with D_2O) ppm; HRMS (ESI-TOF) *m/z* calcd for $C_{19}H_{15}Cl_3F_3N_7O_2S_2$ $[M+H]^+$ 599.9825, found 599.9807. Anal. ($C_{19}H_{15}Cl_3F_3N_7O_2S_2$) C, H, N.

*4.1.1.4. 2-[4-Chloro-5-methyl-2-(naphthalen-1-ylmethylthio)benzenesulfonyl]-1-(4,6-dichloro-1,3,5-triazin-2-ylamino)guanidine (**8**)*

Starting with **4** (1.304 g) and after extraction of impurities with boiling methanol the title compound **8** was afforded 1.398 g (80%): m.p. 182 ºC (dec.); $t_{R=}$ 52.3 min; IR (KBr) ν_{max} 3413, 3315 (N-H); 1648, 1540 (C=C, C=N); 1394, 1236 ($SO_{2\ asym}$); 1131, 1128 ($SO_{2\ sym}$) cm^{-1}; ^1H NMR (500 MHz, DMSO-d_6, 100 ºC) δ 2.33 (s, 3H, CH_3), 4.70 (s, 2H, SCH_2), 6.90 (s, 2H, NH_2), 7.43 (t, 1H, arom), 7.51 (s, 1H, arom), 7.56 (t, 3H arom), 7.86 (d, 1H, arom), 7.88 (s, 1H, arom), 7.92 (d, 1H, arom), 8.23 (d, 1H, arom), 9.38 (s, 1H, NH), 10.76 (s, 1H, NH) ppm; HRMS (ESI-TOF) *m/z* calcd for $C_{22}H_{18}Cl_3N_7O_2S_2$ $[M+H]^+$ 582.0107, found 582.0116. Anal. ($C_{22}H_{18}Cl_3N_7O_2S_2$) C, H, N.

*4.1.2. General procedure for the synthesis of 2-(2-arylmethylthio-4-chloro-5-methylbenzenesulfonyl)-1-(4-chloro-1,3,5-triazin-2-ylamino)guanidines (**9–20**)*

A solution of 2-(2-arylmethylthio-4-chloro-5-methylbenzenesulfonyl)-1-(4,6-dichloro-1,3,5-triazin-2-ylamino)guanidine (0.5 mmol), aminoarylsulfonamide (0.5 mmol) and DIPEA (0.5 mmol) in dry DMF (2 ml) was stirred at 65–80 ºC under an argon atmosphere for 3-11 h. Then the reaction mixture was poured into 50 ml of slush. The solid was filtered off, washed with water, dried under vacuum and purified by crystallization or silica gel chromatography.

*4.1.2.1. 2-(2-Benzylthio-4-chloro-5-methylbenzenesulfonyl)-1-[4-chloro-6-(4-sulfamoylphenylamino)-1,3,5-triazin-2-ylamino]guanidyne (**9**)*

Starting with **5** (0.266 g), 4-aminobenzenesulfonamide (0.090 g), DIPEA (0.086 ml) at 65 ºC for 3 h and after crystallization from toluene/MeOH (v/v = 9:1) the title compound **9** was afforded 0.264 g (79%); m.p. 230–233 ºC; $t_{R=}$ 44.77 min; IR (KBr) ν_{max} 3415, 3329 (NH); 2360 (CH); 1638, 1562 (C=C, C=N); 1340, 1273 ($SO_{2\ asym}$); 1151, 1110 ($SO_{2\ sym}$) cm^{-1}; ^1H NMR (500 MHz, DMSO-d_6, 120 ºC) δ 2.24 (s, 3H, CH_3), 4.19 (s, 2H, SCH_2), 6.87 (s, 2H, NH_2), 7.10 (s, 2H, NH_2), 7.20–7.34 (m, 4H, arom), 7.44 (d, 2H, arom), 7.70–7.94 (m, 5H arom), 8.89 (s, 1H, NH), 9.64 (s, 1H, NH), 10.15 (s, 1H, NH) ppm; HRMS (ESI-TOF) *m/z* calcd for $C_{24}H_{23}Cl_2N_9O_4S_3$ $[M+H]^+$ 668.0490, found 668.0504. Anal. ($C_{24}H_{23}Cl_2N_9O_4S_3$) C, H, N.

*4.1.2.2. 2-[4-Chloro-5-methyl-2-(3-trifluoromethylbenzylthio)benzenesulfonyl]-1-[4-chloro-6-(4-sulfamoylphenylamino)-1,3,5-triazin-2-ylamino]guanidine (**10**)*

Starting with **6** (0.301 g), 4-aminobenzenesulfonamide (0.090 g), DIPEA (0.086 ml) at 65 ºC for 11 h and after crystallization from acetone/water the title compound **10** was afforded 0.258 g (70%); m.p. 150–153 ºC; $t_{R=}$ 41.63 min; IR (KBr) ν_{max} 3325 (N-H); 2360 (CH); 1574

(C=C, C=N); 1331, 1276 ($SO_{2\ asym}$); 1160, 1128,7 ($SO_{2\ sym}$) cm^{-1}; ^1H NMR (500 MHz, DMSO-d_6, 120 ºC) δ 2.23 (s, 3H, CH_3), 4.32 (s, 2H, SCH_2), 6.87 (s, 2H, NH_2), 7.13 (s, 2H, NH_2), 7.29 (s, 1H, arom), 7.40–7.59 (m, 4H, arom), 7.62–7.84 (m, 5H arom), 8.96 (s, 1H, NH), 9.63 (s, 1H, NH), 10.16 (s, 1H, NH) ppm; HRMS (ESI-TOF) *m/z* calcd for $C_{25}H_{22}Cl_2F_3N_9O_4S_3$ $[M+H]^+$ 736.0364, found 736.0373. Anal. ($C_{25}H_{22}Cl_2F_3N_9O_4S_3$) C, H, N.

*4.1.2.3. 2-[4-Chloro-5-methyl-2-(4-trifluoromethylbenzylthio)benzenesulfonyl]-1-[4-chloro-6-(4-sulfamoylphenylamino)-1,3,5-triazin-2-ylamino]guanidine (**11**)*

Starting with **7** (0.300 g), 4-aminobenzenesulfonamide (0.090 g), DIPEA (0.086 ml) at 80 ºC for 6 h and after purification on aluminum oxide using $CHCl_3$/MeOH (v/v = 8 : 1) as the eluent, the title compound **11** was afforded 0.180 g (49%); m.p. 168–171 ºC; $t_{R=}$ 42.38 min; IR (KBr) v_{max} 3314, 2930 (N-H); 2360 (CH); 1619, 1573 (C=C, C=N); 1325, 1275 ($SO_{2\ asym}$); 1158, 1127 ($SO_{2\ sym}$) cm^{-1}; ^1H NMR (500 MHz, DMSO-d_6, 120 ºC) δ 2.27 (s, 3H, CH_3), 4.31 (s, 2H, SCH_2), 6.87 (s, 2H, NH_2), 7.12 (s, 2H, NH_2), 7.31 (s, 1H, arom), 7.57–7.64 (m, 4H, arom), 7.76 (d, 2H, arom), 7.80-7.86 (m, 3H arom), 8.92 (s, 1H, NH), 9.66 (s, 1H, NH), 10.17 (s, 1H, NH) ppm; HRMS (ESI-TOF) *m/z* calcd for $C_{25}H_{22}Cl_2F_3N_9O_4S_3$ $[M+H]^+$ 736.0364, found 736.0374. Anal. ($C_{25}H_{22}Cl_2F_3N_9O_4S_3$) C, H, N.

*4.1.2.4. 2-[4-Chloro-5-methyl-2-(naphthalen-1-ylmethylthio)benzenesulfonyl]-1-[4-chloro-6-(4-sulfamoylphenylamino)-1,3,5-triazin-2-ylamino]guanidine (**12**)*

Starting with **8** (0.291 g), 4-aminobenzenesulfonamide (0.090 g), DIPEA (0.086 ml) at 80 ºC for 8 h and after crystallization from acetone/water the title compound **12** was afforded 0.291 g (81%) m.p. 177–180 ºC; $t_{R=}$ 42.41 min; IR (KBr) v_{max} 3330, 2924 (N-H); 1627, 1564 (C=C, C=N); 1392 (SO_{2asym}); 1157 (SO_{2sym}) cm^{-1}; ^1H NMR (500 MHz, DMSO-d_6, 100 ºC) δ 2.27 (s, 3H, CH_3), 4.66 (s, 2H, SCH_2), 6.95 (s, 2H, NH_2), 7.15 (s, 2H, NH_2), 7.31–7.43 (m, 2H, arom), 7.50–7.60 (m, 4H, arom), 7.65–7.95 (d, 6H, arom), 8.20 (s, 1H, arom), 9.00 (s, 1H, NH), 9.70 (s, 1H, NH), 10.20 (s, 1H, NH) ppm; HRMS (ESI-TOF) *m/z* calcd for $C_{28}H_{25}Cl_2N_9O_4S_3$ $[M+H]^+$ 718.0647, found 718.0673. Anal. ($C_{28}H_{25}Cl_2N_9O_4S_3$) C, H, N.

*4.1.2.5. 2-(2-Benzylthio-4-chloro-5-methylbenzenesulfonyl)-1-[4-chloro-6-(4-sulfamoylphenylmethylamino)-1,3,5-triazin-2-ylamino]guanidine (**13**)*

Starting with **5** (0.266 g), 4-(aminomethyl)benzenesulfonamide hydrochloride (0.111 g), DIPEA (0.172 ml) at 60 ºC for 4 h and after crystallization from $CHCl_3$/EtOH (v/v = 16:3) the title compound **13** was afforded 0.289 g (85%) m.p. 160–164 ºC; $t_{R=}$ 46,25 min; IR (KBr)

v_{max} 3438, 3242 (N-H); 2923, 2852 (CH); 1588, 1553 (C=C, C=N); 1336 (SO_{2asym}); 1159, 1133 (SO_{2sym}) cm^{-1}; ^{1}H NMR (500 MHz, DMSO-d_6, 140 ºC) δ 2.31 (s, 3H, CH_3), 4.22 (s, 2H, SCH_2), 4.48 (s, 2H, $NH\underline{CH_2}$), 6.84 (s, 2H, NH_2), 6.97 (s, 2H, NH_2), 7.23 (t, 1H, arom), 7.30 (t, 2H, arom), 7.35 (s, 1H, arom), 7.38 (d, 2H, arom), 7.45 (d, 2H, arom), 7.79 (d, 2H, arom), 7.85 (s, 1H, arom), 8.16 (s, 1H, NH), 8.73 (s, 1H, NH), 9.16 (s, 1H, NH) ppm; HRMS (ESI-TOF) *m/z* calcd for $C_{25}H_{25}Cl_2N_9O_4S_3$ $[M+H]^+$ 682.0647, found 682.0648. Anal. ($C_{25}H_{25}Cl_2N_9O_4S_3$) C, H, N.

*4.1.2.6. 2-[4-Chloro-5-methyl-2-(3-trifluoromethylbenzylthio)benzenesulfonyl]-1-[4-chloro-6-(4-sulfamoylphenylmethylamino)-1,3,5-triazin-2-ylamino]guanidine (**14**)*

Starting with **6** (0.301 g), 4-(aminomethyl)benzenesulfonamide hydrochloride (0.111 g), DIPEA (0.172 ml) at 80 ºC for 4 h and after purification on silica gel using CH_2Cl_2/ MeOH (v/v = 10 : 0.8) as the eluent, the title compound **14** was afforded 0.100 g (27%) m.p. 140–142 ºC; $t_{R=}$ 42.29 min; IR (KBr) v_{max} 3360 (N-H); 2928 (CH); 1636, 1588 (C=C, C=N); 1396, 1332 (SO_{2asym}); 1130 (SO_{2sym}) cm^{-1}; ^{1}H NMR (500 MHz, DMSO-d_6, 100 ºC) δ 2.29 (s, 3H, CH_3), 4.33 (s, 2H, SCH_2) 4.42 (s, 2H, $NH\underline{CH_2}$), 7.02 (s, 2H, NH_2), 7.09 (s, 2H, NH_2), 7.33 (s, 1H, arom), 7.44 (d, 2H, arom), 7.50–7.58 (m, 2H, arom), 7.68 (d, 2H, arom), 7.77 (d, 2H, arom), 7.84 (s, 1H, arom), 8.36 (s, 1H, NH), 8.90 (s, 1H, NH), 9.36 (s, 1H, NH) ppm; HRMS (ESI-TOF) *m/z* calcd for $C_{26}H_{24}Cl_2F_3N_9O_4S_3$ $[M+H]^+$ 750.0521, found 750.0538. Anal. ($C_{26}H_{24}Cl_2F_3N_9O_4S_3$) C, H, N.

*4.1.2.7. 2-[4-Chloro-5-methyl-2-(4-trifluoromethylbenzylthio)benzenesulfonyl]-1-[4-chloro-6-(4-sulfamoylphenylmethylamino)-1,3,5-triazin-2-ylamino]guanidine (**15**)*

Starting with **7** (0.300 g), 4-(aminomethyl)benzenesulfonamide hydrochloride (0.111 g), DIPEA (0.172 ml) at 80 ºC for 7 h and after purification on silica gel using CH_2Cl_2/MeOH (v/v = 19 : 1) as the eluent, the title compound **15** was afforded 0.240 g (64%) m.p. 158–160 ºC; t_R= 42.78 min; IR (KBr) v_{max} 3332; 2934 (N-H); 1637 (CH); 1587 (C=C, C=N); 1325 (SO_{2asym}); 1130 (SO_{2sym}) cm^{-1}; **1**H NMR (500 MHz, DMSO-d_6, 100 ºC) δ 2.30 (s, 3H, CH_3), 4.33 (s, 2H, SCH_2), 4.44 (s, 2H, $NH\underline{CH_2}$), 7.02 (s, 2H, NH_2), 7.10 (s, 2H, NH_2), 7.35 (s, 1H, arom), 7.45 (d, 2H, arom), 7.55–7.70 (m, 4H, arom), 7.78 (d, 2H, arom), 7.85 (s, 1H arom), 8.36 (s, 1H, NH), 8.89 (s, 1H, NH), 9.38 (s, 1H, NH) ppm; ^{13}C NMR (125 MHz, DMSO-d_6, 23 ºC) δ 19.61, 36.16, 43.78, 126.00, 126.42, 128.16, 128.58, 128.76, 129.53, 130.57, 131.12, 131.28, 132.71, 132.84, 135.51, 137.14, 142.05, 142.23, 143.36, 143.46, 159.08, 166.18,

167.91 ppm; HRMS (ESI-TOF) *m/z* calcd for $C_{26}H_{24}Cl_2F_3N_9O_4S_3$ $[M+H]^+$ 750.0521, found 750.0530. Anal. ($C_{26}H_{24}Cl_2F_3N_9O_4S_3$) C, H, N.

*4.1.2.8. 2-[4-Chloro-5-methyl-2-(naphthalen-1-ylmethylthio)benenesulfonyl]-1-[4-chloro-6-(4-sulfamoylphenylmethylamino)-1,3,5-triazin-2-ylamino]guanidine (**16**)*

Starting with **8** (0.291 g), 4-(aminomethyl)benzenesulfonamide hydrochloride (0.111 g), DIPEA (0.172 ml) at 60 ºC for 8 h and after crystallization from $CHCl_3$/MeOH (v/v = 16:3) the title compound **16** was afforded 0.300 g (82%) m.p. 182 ºC (dec.); $t_{R=}$ 42.59 min; IR (KBr) ν_{max} 3251, 2928 (N-H); 1637, 1585 (C=C, C=N); 1391, 1334 (SO_{2asym}); 1160 (SO_{2sym}) cm^{-1}; ^1H NMR (500 MHz, DMSO-d_6, 100 ºC) δ 2.31 (s, 3H, CH_3), 4.43 (s, 2H, NH$\underline{CH_2}$), 4.69 (s, 2H, SCH_2), 7.02 (s, 2H, NH_2), 7.08 (s, 2H, NH_2), 7.35–7.48 (m, 4H, arom), 7.49–7.65 (m, 3H arom), 7.77 (d, 2H, arom), 7.83–8.03 (m, 3H, arom), 8.22 (d, 1H, arom), 8.35 (s, 1H, NH), 8.88 (s, 1H, NH), 9.34 (s, 1H, NH) ppm; HRMS (ESI-TOF) *m/z* calcd for $C_{29}H_{27}Cl_2N_9O_4S_3$ $[M+H]^+$ 732.0803, found 732.0801. Anal. ($C_{29}H_{27}Cl_2N_9O_4S_3$) C, H, N.

*4.1.2.9. 2-(2-Benzylthio-4-chloro-5-methylbenzenesulfonyl)-1-[4-chloro-6-(3-sulfamoylphenylamino)-1,3,5-triazin-2-ylamino]guanidine (**17**)*

Starting with **5** (0.266 g), 3-aminobenzenesulfonamide (0.090 g), DIPEA (0,086 ml) at 80 ºC for 4.5 h and after purification on silica gel using $CHCl_3$/MeOH (v/v = 8 : 1) as the eluent, the title compound **17** was afforded 0.220 g (66%) m.p. 169–170 ºC; t_R= 39.92 min; IR (KBr) ν_{max} 3341, 3195 (N-H); 2987 (CH); 1648, 1573 (C=C, C=N); 1338, 1274 ($SO_{2\ asym}$); 1130, 1105 ($SO_{2\ sym}$) cm^{-1}; ^1H NMR (500 MHz, DMSO-d_6, 100 ºC) δ 2.27 (s, 3H, CH_3), 4.21 (s, 2H, SCH_2), 7.05 (s, 2H, NH_2), 7.13 (s, 2H, NH_2), 7.23 (t, 1H, arom), 7.28–7.31 (m, 3H, arom), 7.38–7.44 (m, 3H, arom), 7.51 (d, 1H, arom), 7.82 (s, 1H, arom), 8.01 (s, 2H, arom), 8.99 (s, 1H, NH), 9.64 (s, 1H, NH), 10.24 (s, 1 H, NH) ppm; HRMS (ESI-TOF) *m/z* calcd for $C_{24}H_{23}Cl_2N_9O_4S_3$ $[M+H]^+$ 668.0490, found 668.0511. Anal. ($C_{24}H_{23}Cl_2N_9O_4S_3$) C, H, N.

*4.1.2.10. 2-[4-Chloro-5-methyl-2-(3-trifluoromethylbenzylthio)benzenesulfonyl]-1-[4-chloro-6-(3-sulfamoylphenylamino)-1,3,5-triazin-2-ylamino]guanidine (**18**)*

Starting with **6** (0.301 g), 3-aminobenzenesufonamide (0.090 g), DIPEA (0.086 ml) at 80 ºC for 5 h and after purification on silica gel using CH_2Cl_2/MeOH (v/v = 19 : 1) as the eluent, the title compound **18** was afforded 0.191 g (52%) m.p. 137–140 ºC; $t_{R=}$ 42.17 min; IR (KBr) ν_{max} 3316, 2927 (N-H); 2360 (CH); 1559, 1444 (C=C, C=N); 1331 (SO_{2asym}); 1161, 1128 (SO_{2sym}) cm^{-1}; ^1H NMR (500 MHz, DMSO-d_6, 140 ºC) δ 2.28 (s, 3H, CH_3), 4.31 (s, 2H,

SCH_2), 6.87 (s, 2H, NH_2), 7.03 (s, 2H, NH_2), 7.31 (s, 1H, arom), 7.38–7.58 (m, 3H, arom), 7.62–7.71 (m, 3H, arom), 7.84 (s, 1H, arom), 7.97 (s, 1H, arom), 8.05 (s, 1H, arom), 8.87 (s, 1H, NH), 9.44 (s, 1H, NH), 10.03 (s, 1H, NH) ppm; HRMS (ESI-TOF) *m/z* calcd for $C_{25}H_{22}Cl_2F_3N_9O_4S_3$ $[M+H]^+$ 736.0364, found 736.0394. Anal. ($C_{25}H_{22}Cl_2F_3N_9O_4S_3$) C, H, N.

*4.1.2.11. 2-[4-Chloro-5-methyl-2-(4-trifluoromethylbenzylthio)benzenesulfonyl]-1-[4-chloro-6-(3-sulfamoylphenylamino)-1,3,5-triazin-2-ylamino]guanidine (**19**)*

Starting with **7** (0.300 g), 3-aminobenzenesulfonamide (0.090 g), DIPEA (0.086 ml) at 80 ºC for 5 h and after purification on silica gel using CH_2Cl_2/MeOH (v/v = 19 : 1) as the eluent, the title compound **19** was afforded 0.228 g (62%) m.p. 146–149 ºC; $t_{R=}$ 42.30 min; IR (KBr) ν_{max} 3317, 2927 (N-H); 2359 (CH); 1616, 1562 (C=C, C=N); 1389, 1325 (SO_{2asym}); 1160, 1128 (SO_{2sym}) cm^{-1}; ^1H NMR (500 MHz, DMSO-d_6 120 ºC) δ 2.29 (s, 3H, CH_3), 4.32 (s, 2H, SCH_2), 6.98 (s, 2H, NH_2), 7.11 (s, 2H, NH_2), 7.33 (s, 1H arom), 7.43 (t, 1H arom), 7.53 (d, 1H arom), 7.56–7.64 (m, 4H, arom), 7.85 (s, 1H arom), 7.99 (d, 1H arom), 8.04 (s, 1H arom), 8.94 (s, 1H, NH), 9.59 (s, 1H, NH), 10.16 (s, 1H, NH) ppm; HRMS (ESI-TOF) *m/z* calcd for $C_{25}H_{22}Cl_2F_3N_9O_4S_3$ $[M+H]^+$ 736.0364, found 736.0389. Anal. ($C_{25}H_{22}Cl_2F_3N_9O_4S_3$) C, H, N.

*4.1.2.12. 2-[4-Chloro-5-methyl-2-(naphthalen-1-ylmethylthio)benzenesulfonyl]-1-[4-chloro-6-(3-sulfamoylphenylamino)-1,3,5-triazin-2-ylamino]guanidyne (**20**)*

Starting with **8** (0.291 g), 3-aminobenzenesulfonamide (0.090 g), DIPEA (0.086 ml) at 80 ºC for 6 h and after purification on silica gel using CH_2Cl_2/MeOH (v/v = 10 : 0.8) as the eluent, the title compound **20** was afforded 0.179 g (50%) m.p. 157–160 ºC; $t_{R=}$ 37.70 min; IR (KBr) ν_{max} 3325, 2926 (N-H); 2360 (CH); 1625, 1561 (C=C, C=N); 1389, 1274 (SO_{2asym}); 1157, 1110 (SO_{2sym}) cm^{-1}; ^1H NMR (500 MHz, DMSO-d_6, 100 ºC) δ 2.29 (s, 3H, CH_3), 4.67 (s, 2H, SCH_2), 7.06 (s, 2H, NH_2), 7.13 (s, 2H, NH_2), 7.37 (s, 1H, arom), 7.39–7.57 (m, 2H, arom), 7.50–7.57 (m, 4H, arom), 7.83 (d, 1H, arom), 7.86 (s, 1H, arom), 7.90 (d, 1H, arom), 7.95–8.10 (m, 2H, arom), 8.21 (d, 1H, arom), 8.99 (s, 1H, NH), 9.63 (s, 1H, NH), 10.25 (s, 1 H, NH) ppm; HRMS (ESI-TOF) *m/z* calcd for $C_{28}H_{25}Cl_2N_9O_4S_3$ $[M+H]^+$ 718.0647, found 718.0652. Anal. ($C_{28}H_{25}Cl_2N_9O_4S_3$) C, H, N.

4.2. Cell Culture and Cell Viability Assay

All chemicals, if not stated otherwise, were obtained from Sigma-Aldrich (St. Louis, MO, USA). The MCF-7 and HeLa cell lines were purchased from Cell Lines Services (Eppelheim, Germany), the HCT-116 cell line was purchased from ATCC (ATCC-No: CCL-247). Cells were cultured in in Dulbecco's modified Eagle's medium (DMEM) supplemented with 10% fetal bovine serum, 2 mM glutamine, 100 units/ml penicillin, and 100 μg/ml streptomycin. Cultures were maintained in a humidified atmosphere with 5% CO_2 at 37 °C in an incubator (Heraceus, HeraCell).

Cell viability was determined using the MTT (3-(4,5-dimethylthiazol-2-yl)-2,5-diphenyltetrazolium bromide) assay. Cells were seeded in 96-well plates at a density of 5 $\times 10^3$ cells/well and treated for 72 h with the examined compounds in the concentration range 1–100 μM (1, 10, 25, 50 and 100 μM). Following treatment, MTT (0.5 mg/ml) was added to the medium and cells were further incubated for 2 h at 37 °C. Cells were lysed with DMSO and the absorbance of the formazan solution was measured at 550 nm with a plate reader (Victor, 1420 multilabel counter). The optical density of the formazan solution was measured at 550 nm with a plate reader (Victor, 1420 multilabel counter). The experiment was performed in triplicate. Values are expressed as the mean ± SD of at least three independent experiments. Cisplatin used as a positive control presented values of IC_{50}: 2.2 μM, 3.8 μM, 3.0 μM against HeLa, HCT-116 and MCF-7 cells respectively.

4.3. Molecular Dynamics simulations

The Molecular Dynamics (MD) simulations of protein-bound compounds **12** and **20** were based on PDB entries 5DRS (anhydrase II) and 5FL4 (anhydrase IX). The CHARMM36 force field [35] was used for the protein, with zinc-histidine bonded parameters taken from the work by Schmid et al. [36]. Both ligands were parameterized with the CHARMM-compatible CGenFF force field [37], and 4 dihedral angles that joined the rigid planar moieties were parametrized with the M11 DFT functional [38] using the FFTK plugin [39] in VMD. All simulations were performed in Gromacs 5.1 [40] with the Plumed plugin [41]. The systems consisted of a single protein and ligand molecules placed in a periodic dodecahedron box with a cell vector length of 8.86 nm, solvated with 14800 TIP3P water molecules and with K^+ and Cl^- ions added to ensure charge neutrality at the physiological concentration of 0.15 M. Temperature was maintained at 300 K using the velocity rescaling (CSVR) thermostat [42], and pressure at 1 bar using the Berendsen barostat [43]. PME (Particle Mesh Ewald) summation was used for long-range electrostatics [44], and the typical time step of 2 fs was used to integrate the equations of motion.

Based on the structural properties of other anhydrase-sulfonamide complexes available in the literature, the binding mode was assumed to involve the tethering interaction between the zinc-binding catalytic site and the terminal sulfonamide (SO_2NH^-) moiety. Hence, the initial alignment for each of the four possible protein-ligand pairs was performed in individual 100-ns long steered MD (SMD) runs. In SMD, the Zn-N distance was gradually decreased by a semiharmonic potential from 1.0 to 0.19 nm so that the ligand molecule, initially placed in the bulk solvent, was slowly pulled into the binding cavity in the proper orientation.

Since the protein-bound ligand possessed significant conformational freedom, we employed the bias exchange metadynamics (BE-META) enhanced sampling approach [45] to obtain an unbiased ensemble of bound conformations. For each protein-ligand pair, 5 replica simulations were ran for 250 ns, with exchanges attempted every 10 ps. In 4 replicas, metadynamics was performed on individual dihedral angles (the ones that underwent optimization in CGenFF). The fifth replica was unbiased and served to recover the Boltzmann-distributed populations of bound complexes. In all replicas, though, the Zn-N distance was restrained at 0.19 nm to avoid complex dissociation.

To assess the binding affinities of individual trajectory frames, an MM-PBSA calculation was performed on the obtained ensembles of protein-ligand complex configurations using the g_mmpbsa tool [46], as well as short (100 ns) simulations of free protein and free ligand in separate systems.

To ensure that the obtained ensemble is physically meaningful, we performed thermodynamic integration (TI) to confront the estimated difference in affinity between compounds **12** and **20** against the experimental value (2.6 kcal/mol; calculated as $-RTlog\frac{K_1}{K_2}$ based on data from Table 1). To this end, we built a single "alchemical" topology comprising two end states corresponding to the sulfonamide moiety located in meta- (state 0, compound 20) or para- (state 1, compound 1**2**). The λ parameter was used to interpolate between these two states to obtain the free energy difference between states 0 and 1 using the TI equation [47]:

$$\Delta G = \int_0^1 \left\langle \frac{\partial H}{\partial \lambda} \right\rangle d\lambda$$

By performing a set of twenty-four 50-ns replica-exchange simulations of the protein-ligand with values of λ spaced between 0 and 1, and an analogous set of simulations of ligand in water, the difference in affinity, ΔΔG, was estimated using a thermodynamic cycle, i.e. by subtracting the respective transformation free energies in protein complex and in pure solvent.

Clustering was performed on the positions of center of mass (COM) of the naphthyl moiety relative to the binding pocket, as indicative of the overall binding mode. In each case, 4 clusters were produced using the K-means algorithm, and frames closest to cluster centers were used to seed additional 250-ns equilibrium simulations in order to verify the stability of individual binding modes.

Appendix A. Supplementary data

Supplementary data related to this article can be found at http:// dx.doi.org/……

Acknowledgments

This research was supported in part by PL-Grid infrastructure.

References

[1] C.T. Supuran, A. Scozzafava, Angela Casini, Carbonic anhydrase inhibitors, Med. Res. Rev. 23 (2003) 146–189.

[2] S. Pastorekova, S. Parkkila, J. Pastorek, C.T. Supuran, Carbonic anhydrases: current state of the art, therapeutic applications and future prospects, J. Enzyme Inhib. Med. Chem. 19 (2004) 199–229.

[3] C.T. Supuran, Carbonic anhydrases: novel therapeutic applications for inhibitors and activators, Nat. Rev. Drug Discov. 7 (2008) 168–181.

[4] W.M. Eldehna, M. Fares, M. Ceruso, H.A. Ghabbour, S.M. Abou-Seri, H.A. Abdel-Aziz, D.A. Abou El Ella, C.T. Supuran, Amido/ureidosubstituted benzenesulfonamides-isatin conjugates as low nanomolar/subnanomolar inhibitors of the tumor-associated carbonic anhydrase isoform XII. Eur. J. Med. Chem. 110 (2016) 259–266.

[5] F.M. Awadallah, T.A. El-Waei, M.M. Hanna, S.E. Abbas, M. Ceruso, B.E. Oz, O.O. Guler, C.T. Supuran, Synthesis, carbonic anhydrase inhibition and cytotoxic activity of novel chromone-based sulfonamide derivatives. Eur. J. Med. Chem. 96 (2015) 425–435.

[6] M. Leppilampi, J. Saarnio, T.J. Karttunen, J. Kivelä, S. Pastoreková, J. Pastorek, A. Waheed, W.S. Sly, S. Parkkila, Carbonic anhydrase isozymes IX and XII in gastric tumors. World J. Gastroenterol. 9 (2003) 1398–1403.

[7] S. Pastoreková, S. Parkkila, A.K. Parkkila, R. Opavský, V. Zelník, J. Saarnio, J. Pastorek, Carbonic anhydrase IX, MN/CA IX: analysis of stomach complementary DNA sequence and expression in human and rat alimentary tracts, Gastroenterology 112 (1997) 398–408.

[8] K. Nordfors, J. Haapasalo, M. Korja, A. Niemelä, J. Laine, A.K. Parkkila, S. Pastorekova, J. Pastorek, A. Waheed, W.S. Sly, S. Parkkila, H. Haapasalo, The tumour-associated carbonic anhydrases CA II, CA IX and CA XII in a group of medulloblastomas and supratentorial primitive neuroectodermal tumours: an association of CA IX with poor prognosis. BMC Cancer. 10 (2010) 148.

[9] E. Svastova, N. Zilka, M. Zatovicova, A. Gibadulinova, F. Ciampor, J. Pastorek, S. Pastorekova, Carbonic anhydrase IX reduces E-cadherin-mediated adhesion of MDCK cells via interaction with beta-catenin. Exp. Cell Res. 290 (2003) 332–345.

[10] E. Svastova, W. Witarski, L. Csaderova, I. Kosik, L. Skvarkova, A. Hulikova, M. Zatovicova, M. Barathova, J. Kopacek, J. Pastorek, S. Pastorekova, Carbonic Anhydrase IX Interacts with Bicarbonate Transporters in Lamellipodia and Increases Cell Migration via Its Catalytic Domain. J. Biol. Chem. 287 (2012) 3392–3402.

[11] C.C. Wykoff, N.J. Beasley, P.H. Watson, K.J. Turner, J. Pastorek, A. Sibtain, G.D. Wilson, H. Turley, K.L. Talks, P.H. Maxwell, C.W. Pugh, P.J. Ratcliffe, A.L. Harris, Hypoxia-inducible expression of tumor-associated carbonic anhydrases, Cancer Res. 60 (2000) 7075–7083.

[12] P. Ditte, F. Dequiedt, E. Svastova, A. Hulikova, A. Ohradanova-Repic, M. Zatovicova, L. Csaderova, J. Kopacek, C.T. Supuran, S. Pastorekova, J. Pastorek, Phosphorylation of carbonic anhydrase IX controls its ability to mediate extracellular acidification in hypoxic tumors. Cancer Res. 71 (2011) 7558–7567.

[13] D. Neri, C.T. Supuran, Interfering with pH regulation in tumours as a therapeutic strategy, Nat. Rev. Drug Discov. 10 (2011) 767–777.

[14] Y. Lou, P.C. McDonald, A. Oloumi, S. Chia, C. Ostlund, A. Ahmadi, A. Kyle, U. Auf dem Keller, S. Leung, D. Huntsman, B. Clarke, B.W. Sutherland, D. Waterhouse, M. Bally, C. Roskelley, C.M. Overall, A. Minchinton, F. Pacchiano, F. Carta, A. Scozzafava, N. Touisni, J.Y. Winum, C.T. Supuran, S. Dedhar, Targeting tumor hypoxia: suppression of

breast tumor growth and metastasis by novel carbonic anhydrase IX inhibitors, Cancer Res. 71 (2011) 3364–3376.

[15] K. DeClerck, R.C. Elble, The role of hypoxia and acidosis in promoting metastasis and resistance to chemotherapy, Front. Biosci. 15 (2010) 213–225.

[16] W.J. Huang, Y.M. Jeng, H.S. Lai, I.U. Fong, F.Y. Sheu, P.L. Lai, R.H. Yuan. Expression of hypoxic marker carbonic anhydrase IX predicts poor prognosis in resectable hepatocellular carcinoma. PLoS One (2015) doi: 10.1371/journal.pone.0119181

[17] Potter C, Harris AL: Hypoxia inducible carbonic anhydrase IX, marker of tumor hypoxia, survival pathway and therapy target. Cell Cycle. 2004, 3 (2): 164–167.

[18] C.T. Supuran, Carbonic anhydrase inhibitors. Bioorg. Med. Chem. Lett. 20 (2010) 3467–3474.

[19] A. Thiry, J.M. Dogné, B. Masereel, C.T. Supuran, Targeting tumor-associated carbonic anhydrase IX in cancer therapy. Trends Pharmacol. Sci. 27 (2006) 566–573.

[20] C.T. Supuran. Inhibition of carbonic anhydrase IX as a novel anticancer mechanism. World J. Clin. Oncol. 3 (2012) 98–103.

[21] A. Mollica, R. Costante, A. Akdemir, S. Carradori, A. Stefanucci, G. Macedonio, M. Ceruso, C.T. Supuran. Exploring new Probenecid-based carbonic anhydrase inhibitors: Synthesis, biological evaluation and docking studies. Bioorg. Med. Chem. 23 (2015) 5311–5318.

[22] E. Paolicchi, F. Gemignani, M. Krstic-Demonacos, S. Dedhar, L. Mutti, S. Landi. Targeting hypoxic response for cancer therapy. Oncotarget. 7 (2016) 13464–1378.

[23] V. Garaj, L. Puccetti, G. Fasolis, J.Y. Winum, J.L. Montero, A. Scozzafava, D. Vullo, A. Innocenti, C.T. Supuran, Carbonic anhydrase inhibitors: synthesis and inhibition of cytosolic/tumor-associated carbonic anhydrase isozymes I, II, and IX with sulfonamides incorporating 1,2,4-triazine moieties. Bioorg. Med. Chem. Lett. 14 (2004) 5427–5433.

[24] V. Garaj, L. Puccetti, G. Fasolis, J.Y. Winum, J.L. Montero, A. Scozzafava, D. Vullo, A. Innocenti, C.T. Supuran, Carbonic anhydrase inhibitors: Novel sulfonamides incorporating

1,3,5-triazine moieties as inhibitors of the cytosolic and tumor-associated carbonic anhydrase isozymes I, II and IX, Bioorg. Med. Chem. Lett. 15 (2005) 3102–3108.

[25] F. Carta, V. Garaj, A. Maresca, J. Wagner, B.S. Avvaru, A.H. Robbins, A. Scozzafava, R. McKenna, C.T. Supuran, Sulfonamides incorporating 1,3,5-triazine moieties selectively and potently inhibit carbonic anhydrase transmembrane isoforms IX, XII and XIV over cytosolic isoforms I and II: Solution and X-ray crystallographic studies. Bioorg. Med. Chem. 19 (2011) 3105–3119.

[26] J. Sławiński, A. Pogorzelska, B. Żołnowska, K. Brożewicz, D. Vullo, C.T. Supuran, Carbonic anhydrase inhibitors. Synthesis of a novel series of 5-substituted 2,4-dichlorobenzenesulfonamides and their inhibition of human cytosolic isozymes I and II and the transmembrane tumor-associated isozymes IX and XII. Eur. J. Med. Chem. 82 (2014) 47–55.

[27] J. Sławiński, Z. Brzozowski, B. Żołnowska, K. Szafrański, A. Pogorzelska, D. Vullo, C.T. Supuran, Synthesis of a new series of N^4 -substituted 4-(2-aminoethyl)benzenesulfonamides and their inhibitory effect on human carbonic anhydrase cytosolic isozymes I and II and transmembrane tumor-associated isozymes IX and XII. Eur. J. Med. Chem. 84 (2014) 59–67.

[28] B. Żołnowska, J. Sławiński, A. Pogorzelska, J. Chojnacki, D. Vullo, C.T. Supuran, Carbonic anhydrase inhibitors. Synthesis, and molecular structure of novel series *N*-substituted *N*'-(2-arylmethylthio-4-chloro-5-methylbenzenesulfonyl)guanidines and their inhibition of human cytosolic isozymes I and II and the transmembrane tumor-associated isozymes IX and XII. Eur. J. Med. Chem. 71 (2014) 135–147.

[29] J. Sławiński, Syntheses and some reactions of 3-amino-6-chloro-7-methyl-1,1-dioxo-1,4,2-benzodithiazine. Polish J. Chem. 75 (2001) 1309–1316.

[30] J. Sławiński, A. Pogorzelska, B. Żołnowska, A. Kędzia, M. Ziółkowska-Klinkosz, E. Kwapisz, Synthesis and anti-yeast evaluation of novel 2-alkylthio-4-chloro-5-methyl-*N*-[imino-(1-oxo-(1*H*)-phthalazin-2-yl)methyl]benzenesulfonamide derivatives. Molecules 19 (2014) 13704–13723.

[31] B. Żołnowska, J. Sławiński, A. Pogorzelska, K. Szafrański, A. Kawiak, G. Stasiłojć, M. Belka, S. Ulenberg, T. Bączek, J. Chojnacki, Novel 5-Substituted 2-(Aylmethylthio)-4-chloro-*N*-(5-aryl-1,2,4-triazin-3-yl)benzenesulfonamides: Synthesis, Molecular Structure, Anticancer Activity, Apoptosis-Inducing Activity and Metabolic Stability. Molecules 21 (2016) 808.

[32] A. Zubriene, A. Smirnov, V. Dudutienė, D.D. Timm, J. Matulienė, V. Michailovienė, A. Zakšauskas, E. Manakova, S. Gražulis, D. Matulis, Intrinsic Thermodynamics and Structures of 2,4- and 3,4-Substituted Fluorinated Benzenesulfonamides Binding to Carbonic Anhydrases. Chem. Med. Chem. 12 (2017) 161–176.

[33] J. Leitans, A. Kazaks, A. Balode, J. Ivanova, R. Zalubovskis, C.T. Supuran, K. Tars K, Efficient Expression and Crystallization System of Cancer-Associated Carbonic Anhydrase Isoform IX. J. Med. Chem. 58 (2015) 9004–9009.

[34] V. Dudutienė, J. Matulienė, A. Smirnov, D.D. Timm, A. Zubrienė, L. Baranauskienė, V. Morkūnaite, J. Smirnovienė, V. Michailovienė, V. Juozapaitienė, A. Mickevičiūtė, J. Kazokaitė, S. Bakšytė, A. Kasiliauskaitė, J. Jachno, J. Revuckienė, M. Kišonaitė, V. Pilipuitytė, E. Ivanauskaitė, G. Milinavičiūtė, V. Smirnovas, V. Petrikaitė, V. Kairys, V. Petrauskas, P. Norvaišas, D. Lingė, P. Gibieža, E. Capkauskaitė, A. Zakšauskas, E. Kazlauskas, E. Manakova, S. Gražulis, J.E. Ladbury, D. Matulis, Discovery and characterization of novel selective inhibitors of carbonic anhydrase IX. J. Med. Chem. 57 (2014) 9435–9446.

[35] R.B. Best, X. Zhu, J. Shim, P.E. Lopes, J. Mittal, M. Feig, A.D. Mackerell Jr, Optimization of the additive CHARMM all-atom protein force field targeting improved sampling of the backbone φ, ψ and side-chain χ(1) and χ(2) dihedral angles. J. Chem. Theory Comput. 8 (2012) 3257–3273.

[36] N.M. Kidwell, D.N. Mehta-Hurt, J.A. Korn, E.L. Sibert, T.S. Zwier, Ground and excited state infrared spectroscopy of jet-cooled radicals: exploring the photophysics of trihydronaphthyl and inden-2-ylmethyl. J. Chem. Phys. 140 (2014) 214302.

[37] K. Vanommeslaeghe, E. Hatcher, C. Acharya, S. Kundu, S. Zhong, J. Shim, E. Darian, O. Guvench, P. Lopes, I. Vorobyov, A. D. Mackerell Jr. CHARMM general force field: A

force field for drug-like molecules compatible with the CHARMM all-atom additive biological force fields. J. Comp. Chem. 31 (2010) 671–690.

[38] R. Peverati, D.G. Truhlar, Improving the Accuracy of Hybrid Meta-GGA Density Functionals by Range Separation. J. Phys. Chem. Lett. 2 (2011) 2810–2817.

[39] C.G. Mayne, J. Saam, K. Schulten, E. Tajkhorshid, J.C. Gumbart, Rapid parameterization of small molecules using the Force Field Toolkit. J. Comput. Chem. 34 (2013) 2757–2770.

[40] M.J. Abraham, T. Murtola, R. Schulz, S. Páll, J.C. Smith, B. Hess, E. Lindahl, GROMACS: High performance molecular simulations through multi-level parallelism from laptops to supercomputers. SoftwareX 1 (2015) 19–25.

[41] G.A. Tribello, M. Bonomi, D. Branduardi, C. Camilloni, G. Bussi, PLUMED 2: New feathers for an old bird. Comp. Phys. Comm. 185 (2014) 604–613.

[42] G. Bussi, D. Donadio, M. Parrinello, Canonical sampling through velocity rescaling. J. Chem. Phys. 126 (2007) 014101.

[43] H. J. C. Berendsen, J. P. M. Postma, W. F. van Gunsteren, A. DiNola, and J. R. Haak, Molecular dynamics with coupling to an external bath. J. Chem. Phys. 81 (1984) 3684.

[44] T. Darden, D. York, L. Pedersen, Particle mesh Ewald: An N·log(N) method for Ewald sums in large systems. J. Chem. Phys. 98 (1993) 10089.

[45] S. Piana, A. Laio, A bias-exchange approach to protein folding. J. Phys. Chem. B. 111 (2007) 4553–4559.

[46] R. Kumari, R. Kumar, Open Source Drug Discovery Consortium, Lynn A, g_mmpbsa--a GROMACS tool for high-throughput MM-PBSA calculations. J. Chem. Inf. Model. 54 (2014) 1951-1962.

[47] J.A. Barker, D. Henderson, What is "liquid"? Understanding the states of matter. Rev. Mod. Phys. 48 (1976) 587.

Figure and scheme captions

Click here to view linked References

Fig. 1. General structures of clinically used sulfonamides **AAZ, MZA, DCP** and **EZA** (standard CA inhibitors) and sulfonamide SLC-0111, being in clinical trials.

Fig 2. Structures of benzenesulfonamides **A**, **B**, **C, D** and **E**.

Fig. 3. (**A**) The binding poses identified for compound **12** by the clustering procedure, with cluster centers (shown in the stick representation) and cluster members (shown as transparent spheres corresponding to the position of the naphthyl moiety). (**B**) Stability of identified binding poses in 250 ns equilibrium simulations. Fewer transitions between unstable poses correlate with higher affinity as determined experimentally. (**C**) Difference in binding enthalpy between compound **12** and the corresponding (according to the BLAST alignment) amino acids of hCA IX and II, mapped onto the protein structure. Red indicates higher binding enthalpy in case of hCA IX, blue – in case of hCA II.

Scheme 1. Scheme 1. Synthesis of 2-(2-arylmethylthio-4-chloro-5-methylbenzenesulfonyl)-1-(1,3,5-triazin-2-ylamino)guanidine **5-8** and **9-20**. Reagents and conditions: a) 2,4,6-trichloro-1,3,5-triazine (1 equiv.), TEA (1-2 equiv.), anhydrous THF, 1 h at 0 °C, 2 h at r.t.; b) X-NH_2 (1 equiv.), DIPEA (1 equiv.), 80°C, argon atmosphere, 3–11 h.

Fig. S1. Cluster number optimization. The plot shows the K-Means objective calculated for different choices of cluster number. For hCA II and hCA IX the elbow method suggests that the optimal number of clusters is 3 and 4, respectively, so that the existence of 4 clusters were assumed in both cases for consistency.

Fig. S2. Sample modes of interaction between Arg64 of hCA IX (blue) and compound **12** (yellow) assumed during enhanced sampling simulations. (**A**) The naphthyl ring stacks on top of the guanidine moiety. (**B**) Arg64 fits in a cleft on the surface of compound **12**, interacting with the sulfonamide moiety *via* hydrogen bonds and forming hydrophobic/π-π contacts with the naphthyl ring. (**C**) Naphthyl and guanidine interact in a side-to-side arrangement. (**D**) The phenyl ring stacks on top of the guanidine moiety.

Table 1. Carbonic anhydrase inhibition data for compounds **9-20** and standard inhibitors against human isozymes hCA I, II, IX and XII by a stopped-flow CO_2 hydrase assay.

Compound	R	X	K_I[a] (nM)			
			hCA I	hCA II	hCA IX	hCA XII
AAZ			250	12.1	25.8	5.7
MZA			780	14	27	3.4
EZA			25	8	34	22
DCP			1200	38	50	50
9	Ph	4-$(H_2NSO_2)C_6H_4$	66.6	83.7	39.4	31.1
10	3-$CF_3C_6H_4$	4-$(H_2NSO_2)C_6H_4$	147.6	7.4	37.1	91.9
11	4-$CF_3C_6H_4$	4-$(H_2NSO_2)C_6H_4$	385.6	22.0	42.9	87.5
12	1-naphthyl	4-$(H_2NSO_2)C_6H_4$	733.3	160.8	41.1	77.6
13	Ph	4-$(H_2NSO_2)C_6H_4CH_2$	294.2	38.8	46.9	78.8
14	3-$CF_3C_6H_4$	4-$(H_2NSO_2)C_6H_4CH_2$	218.9	5.4	43.6	255.5
15	4-$CF_3C_6H_4$	4-$(H_2NSO_2)C_6H_4CH_2$	513.8	89.5	47.1	183.3
16	1-naphthyl	4-$(H_2NSO_2)C_6H_4CH_2$	2141.0	186.9	383.0	73.4
17	Ph	3-$(H_2NSO_2)C_6H_4$	395.9	94.7	3968.7	64.6
18	3-$CF_3C_6H_4$	3-$(H_2NSO_2)C_6H_4$	336.8	9.3	3342.1	225.8
19	4-$CF_3C_6H_4$	3-$(H_2NSO_2)C_6H_4$	536.1	326.2	421.1	392.8
20	1-naphthyl	3-$(H_2NSO_2)C_6H_4$	3341.0	933.1	3403.2	337.9

[a] Mean from 3 different determinations (errors were in the range of ±5-10% of the reported values, data not shown).

Figure S1

Click here to download high resolution image

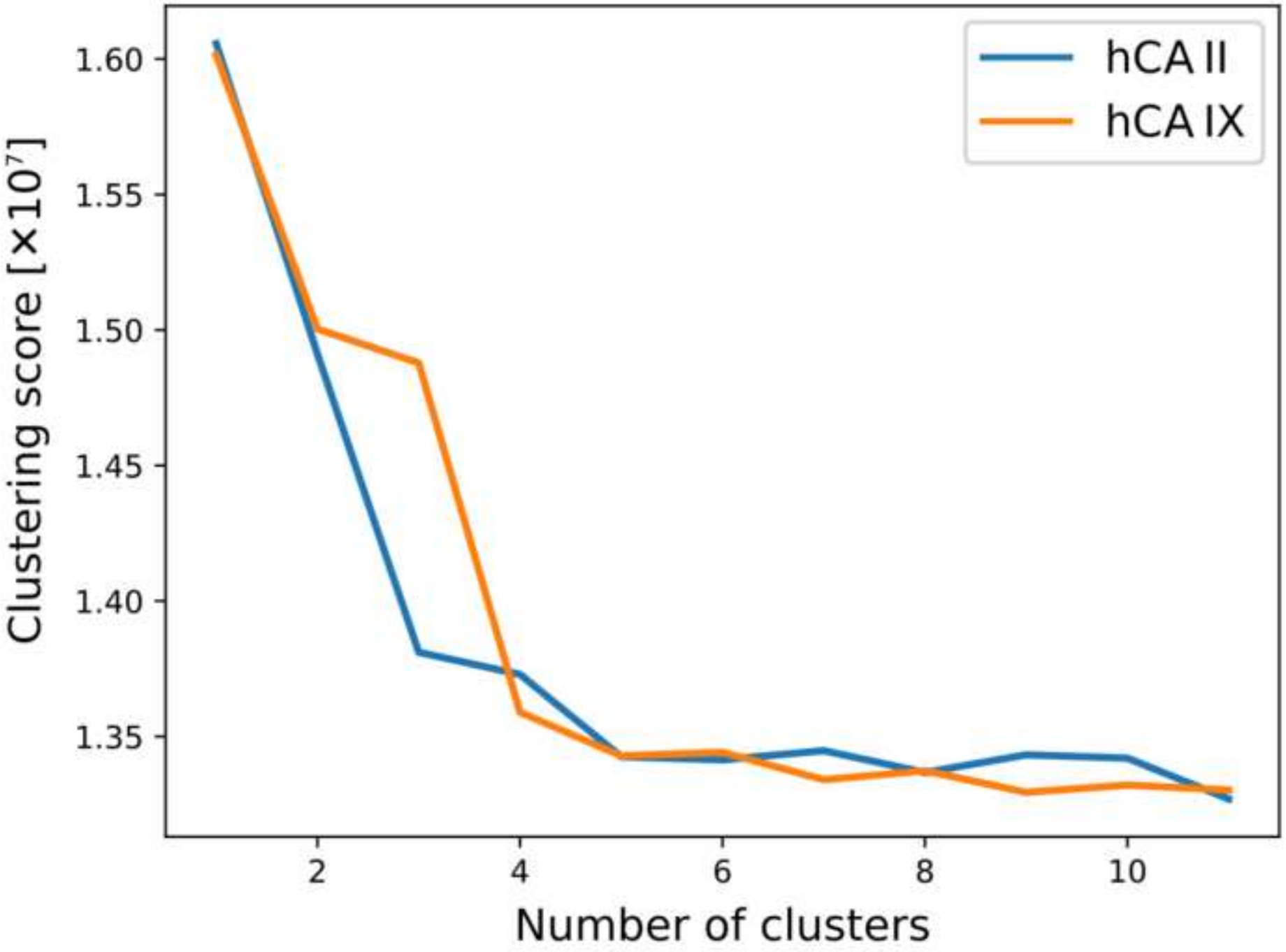

Figure S2

Click here to download high resolution image

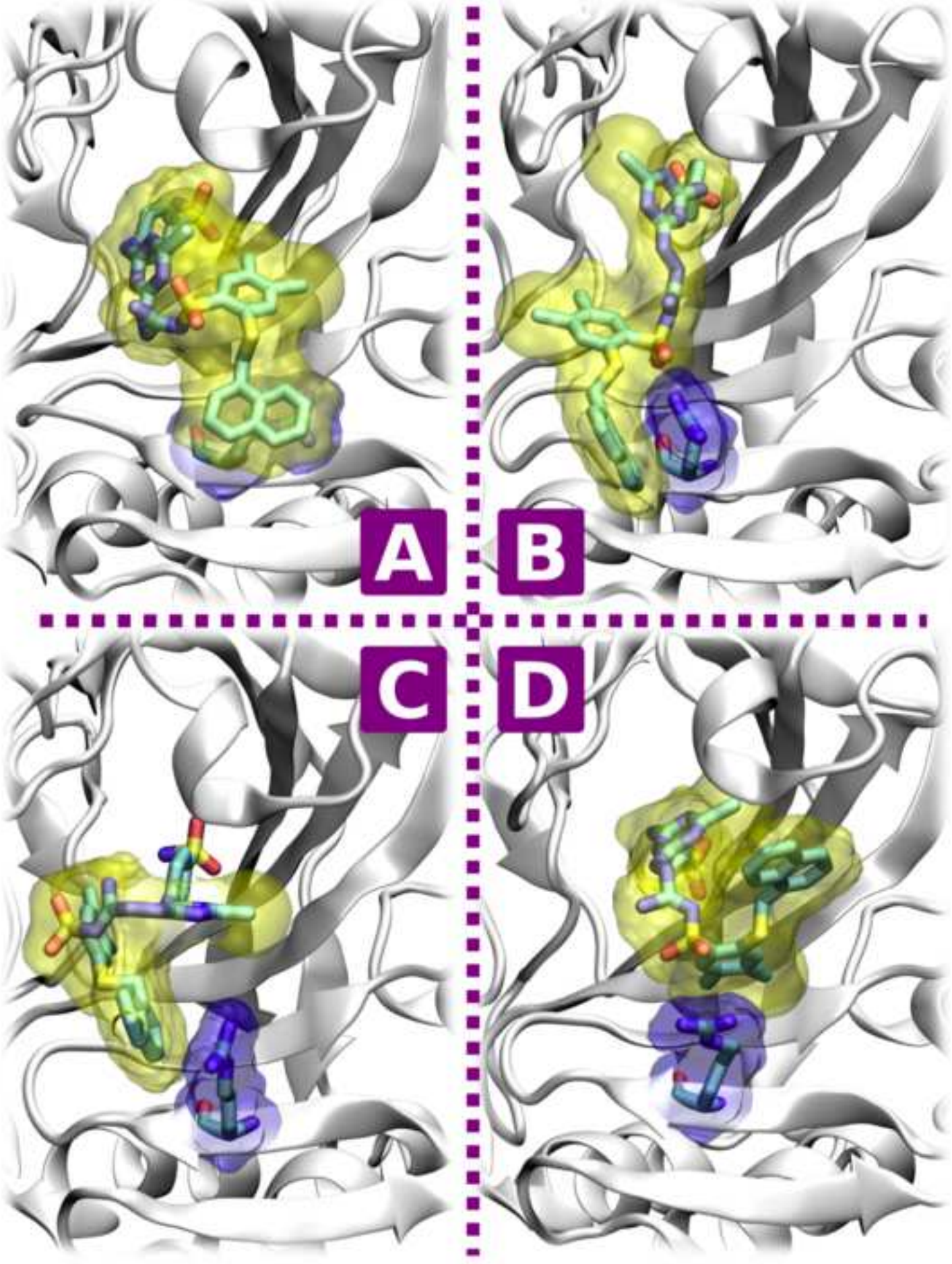

Figure 3

Click here to download high resolution image